CLM-P600

CLM-P600

UKAEA

Preprint

THE INTERPRETATION OF AXISYMMETRIC JUMPS IN A HEXAPOLE TOKAMAK

F. A. HAAS
A. J. WOOTTON

CULHAM LABORATORY
Abingdon Oxfordshire

1980

CLM-P 600

THE INTERPRETATION OF AXISYMMETRIC JUMPS IN A HEXAPOLE TOKAMAK

F.A. Haas and A.J. Wootton

Culham Laboratory, Abingdon, Oxon., OX14 3DB, UK
(Euratom/UKAEA Fusion Association)

ABSTRACT

Experiments on a small tokamak, TOSCA, have shown that a hexapole magnetic field produces axisymmetric jumps in major radius. These occur when the hexapole field is used to produce an outward pointing triangular deformation to the plasma cross-section. A theoretical model is presented which interprets these jumps as the transition between two equilibrium states following a perturbation to the plasma parameters, for example, the self-inductance per unit length and poloidal beta. The model predicts the magnitude of the jump as a function of the hexapole field and the initial plasma position.

(Submitted for publication in Nuclear Fusion)

October 1979

1. INTRODUCTION

Triangular distortions to the plasma cross-section in a tokamak have been proposed as a method of improving MHD stability[1] and producing an axisymmetric divertor. The TOSCA experiment has been used to study the equilibrium, stability and confinement properties of such plasmas.[2] In this machine, the equilibrium is maintained by preprogrammed fields, rather than by induced currents or an active feedback control system. When a hexapole magnetic field is applied to make an outward pointing triangular deformation, axisymmetric jumps in major radius are observed. Displacements of up to 3 cm (for a minor radius of 8 cm and a major radius of 30 cm) occur in times between 10 and 100 μs; the motion does not appear to be exponential. It should be noted, that the jump having occurred, there are no subsequent oscillations of the plasma; this damping is presumably due to the high effective resistance of the vacuum vessel (time constant of order 7 μs). The jumps restrict the triangularity of the plasma, because once the plasma has moved from the centre of the hexapole, the plasma distortion becomes predominantly elliptic. Following the jump, contact with material surfaces increases the impurity concentration, so that it is impossible to produce an outward pointing plasma of the required triangularity and purity for stability and confinement studies. The restrictions on the production and major radial positioning, R_p, of such a plasma can be best inferred from Fig. 1. Defining the hexapole and toroidal plasma currents to be I_h and I_p, respectively, then the figure indicates the region in $\left(\frac{I_h}{I_p}, R_p\right)$ parameter space available for producing outward pointing triangular plasmas; a detailed discussion of this figure is given in a later section. Both circular and inward pointing plasmas also exhibit jumps but these are much smaller, typically a few millimeters. This paper catalogues the experimental results associated with the jumps, and then attempts to interpret them in terms of a simple theory.

Suppose we represent a hexapole field by six straight conductors carrying the same current and placed symmetrically with respect to each other. Treating the plasma as a wire, there is only one position of equilibrium, that is, at the centre of the configuration. If, however, we allow a small error in the current carried by one of the conductors, then two equilibrium positions now arise, one of which is unstable. This simple example suggests that we investigate a model which represents the TOSCA field as closely as possible. Assuming the plasma cross-section to be near circular, we use Shafranov's well known formula[3] to relate the plasma current (I_p) and major radial position (R_p) to the magnetic field required for equilibrium; the latter results from all components of the TOSCA field. The formula also involves the plasma minor radius (a) and the plasma parameters, namely, the self-inductance per unit length and the poloidal beta.

The interpretation which we present assumes that the plasma jump is the transition between an initial equilibrium (state 1) and a final equilibrium (state 2). We can envisage two possibilities. First, that there is a second equilibrium in the neighbourhood of state 1, and that an appropriate change in plasma current and parameters will enable this second equilibrium to be reached. Alternatively, a change in I_p and parameters leads to a modification of the initial equilibrium. In either case we shall describe the final equilibrium as state 2. The initial analysis assumes that during the jump the magnetic flux is conserved, and this, together with the circuit, determines the change in the toroidal plasma current. Subsequent consideration of the energetics leads us to the conclusion that poloidal flux is lost. We also assume that the motion is adiabatic and that particles are conserved.

We shall make no attempt to describe the detailed processes which give rise to the jumps - only to discuss the possible equilibrium states available to the plasma.

The question does arise however, as to the trigger mechanism responsible for the jump. It seems reasonable to suppose that the essential effect is due to a redistribution of current within the plasma, and observation indicates two possible sources of stimulus. First, some jumps are preceded by low-level fluctuations in the poloidal field, and these can be plausibly attributed to the m = 2 tearing-mode. Second, a change in the primary voltage (due to the switching of capacitance) can also stimulate a jump. By suitably choosing the trigger mechanism we can match the experimental and theoretical results. Our model predicts the dependence of the jump on the triangularity (magnitude of hexapole field) and the initial plasma position. We find good agreement except for jumps which start from initial positions on the inside of the vessel centre.

2. THEORY

(a) Equilibrium

Using MKS units and defining a and R_p to be the respective minor and major radii of the plasma, then the vertical field B_z required to maintain equilibrium in the limit $a/R_p \ll 1$, is[3]

$$B_z = -\frac{\mu_o I_p}{4\pi R_p}\Phi \qquad \text{... (1)}$$

where I_p is the total toroidal plasma current, and

$$\Phi = \ell n\left(\frac{8R_p}{a}\right) + \beta_I + \frac{\ell_i}{2} - 3/2. \qquad \text{... (2)}$$

The poloidal beta, β_I, is defined to be

$$\beta_I = \frac{2\mu_o \langle p \rangle}{B_\theta{}^2(a)} \qquad \text{... (3)}$$

where <p> denotes the pressure averaged over the cross-section, and $B_\theta(a)$ is the poloidal field at the plasma surface due to I_p. The inductance per unit length, $\frac{\mu_o \ell_i}{4\pi}$, is defined as

$$\ell_i = 2\int_o^a B_\theta^2 \, rdr/(B_\theta^2(a)a^2) \qquad \text{... (4)}$$

We note that Eq(1) was originally derived for circular plasmas in homogeneous fields. Numerical calculations[(4)] for TOSCA, however, demonstrate the formula to be very accurate for non-circular plasmas in situations where the field is markedly inhomogeneous; the minor radius, a, now representing an average value.

In TOSCA, equilibrium is maintained by a field which results from several different components (see Fig. 2). The dominant component arises from the background vertical field, B_z^{vert} (Fig. 2a), and which is proportional to R^{-n}, n being the decay index. In order to ascertain the R-dependence of the hexapole field, we replace the actual windings by six conductors situated symmetrically with respect to $(R_o, 0)$, the point at which the hexapole field vanishes. If these conductors are distance d from $(R_o, 0)$ and carry the same current I_h, then it is straightforward to show that

$$B_z^{hex} = \frac{\mu_o}{4\pi} \frac{12\ I_h R_o^2}{d^3} \left(R/R_o - 1\right)^2 \equiv B_z^h \left(R/R_o - 1\right)^2 \quad \ldots (5)$$

where we have assumed $a \ll d \ll R_p$. In using the above formula, we shall substitute a value for B_z^h determined from the experiment. Equation (5), however, is only approximately representative of the experimental hexapole field. The most significant departure is proportional to $(R - R_o)$, that is, a quadrupole effect, and which we write as

$$B_z^{error} = B_z^e\ (R/R_o - 1). \quad \ldots (6)$$

This component is essential if the correct plasma configurations are to be reproduced. Figs. 2b and 2c show plots of B_z^{hex} and B_z^{error}, respectively. Figure 2d shows the sum of the individual fields which comprise the total vertical field, B_z. The difference between the model (solid curve) and the actual field (broken curve) is due to a further component arising from the primary winding.

We assume the plasma to occupy an initial equilibrium (state 1) with major and minor radii, a_1 and R_{p1}, respectively, where

$$B_{z1} = B_{z1}^{vert} + B_{z1}^{hex} + B_{z1}^{error} = - \frac{\mu_o I_{p1}}{4\pi R_{p1}} \Phi_1. \quad \ldots (7)$$

As described in the introduction, two possibilities can occur. First, that there is a second equilibrium in the neighbourhood of state 1, and that a suitable change in plasma parameters and current will enable the system to move to this equilibrium. Alternatively, changes in plasma parameters and current lead to a modification of the initial equilibrium. In either case, the final equilibrium will be referred to as state 2. Assuming the separation between states to be small, we write $R_{p2} - R_{p1} = \Delta R$ and suppose $R_{p1} - R_o \sim \Delta R$. Now for the processes envisaged, the change in Φ between states can be expressed as

$$\Delta\Phi = \alpha + \chi \frac{\Delta R}{R_{p1}}, \qquad \ldots (8)$$

where assuming flux conservation, for example, α can be shown to depend on the change in inductance per unit length ($\Delta\ell_i$), and χ to involve β_I (see part (b) of this section). We take the toroidal current to change according to the relation

$$\frac{\Delta I_p}{I_{p1}} = - \lambda \frac{\Delta R}{R_{p1}} \qquad \ldots (9)$$

where the parameter λ may be directly inferred from experiment, or, assuming flux conservation, an expression for λ can be derived in terms of the various equilibrium quantities (see part (c)).

Expanding in $\Delta R/R_o$ and retaining terms to leading-order only, Eqs (5)-(9) yield the result

$$A\left(\frac{\Delta R}{R_o}\right)^2 + B\left(\frac{\Delta R}{R_o}\right) + C = 0, \qquad \ldots (10)$$

where
$$A = B_z^h/B_{z1}^{vert} \qquad \ldots (11)$$

$$B = 1 + \lambda - \frac{\chi}{\Phi_1} + \frac{2B_z^h}{B_{z1}^{vert}}(R_{p1}/R_o - 1) + \frac{B_z^e}{B_{z1}^{vert}} - n \qquad \ldots (12)$$

and
$$C = - \frac{\alpha}{\Phi_1}. \qquad \ldots (13)$$

We note that all terms involving $(\Delta R/R_o)^2$ have been neglected with the exception of those arising from the hexapole field. For the latter, substitution of typical experimental values shows them to be comparable with terms linear in $\Delta R/R_o$. Thus we obtain

$$\frac{\Delta R}{R_o} = -\frac{B}{2A}\left[1 \pm \left(1 - \frac{4AC}{B^2}\right)^{\frac{1}{2}}\right] \qquad \ldots (14)$$

and observe that two solution are possible. That corresponding to the negative sign is essentially due to a modification of the initial state, while the positive sign refers to a neighbouring equilibrium. Switching off the hexapole field ($B_z^h \to 0$) clearly demonstrates these two solutions. Thus for the first, $\frac{\Delta R}{R_o} = -\frac{C}{B}$, whilst the second is at infinity, that is, outside the vacuum vessel. As the hexapole field is re-applied, the second solution moves inwards and eventually neighbours the initial state. We note that the derivation of Eq (14) does not depend on flux conservation.

Although we are specifically concerned to explain the observations in TOSCA, the above theory is in fact applicable to any configuration in which the vertical field in the vicinity of the plasma can be expressed in the form

$$B_z = L + M\frac{\Delta R}{R_o} + N\left(\frac{\Delta R}{R_o}\right)^2 \qquad \ldots (15)$$

where L, M (ellipticity) and N (triangularity) are constants corresponding to a particular equilibrium.

Development of our theory to higher order in $\frac{\Delta R}{R}$ could lead to yet further equilibria. Thus it is possible that the solutions found in Eq (14) are both stable.

(b) <u>Change in Plasma Parameters</u>

Assuming flux conservation, we now express α and χ in terms of changes in the plasma parameters. During any transition

$$a^2\bar{B}_\phi = \text{constant}, \qquad \ldots (16)$$

where $\bar{B}_\phi$ is the mean toroidal field within the plasma. For conditions in TOSCA, $\bar{B}_\phi$ is essentially the vacuum field, and hence

$$\bar{B}_\phi \propto 1/R. \qquad \ldots (17)$$

It follows from Eqs (16) and (17) that

$$\frac{\Delta a}{a_1} = \frac{\Delta R}{2R_{p1}}. \qquad \ldots (18)$$

Defining $\bar{p}$ to be the mean pressure within the plasma and assuming changes to occur adiabatically, then

$$\bar{p} \propto a^{-10/3} R^{-5/3}. \qquad \ldots (19)$$

Using the above relations together with Eqs (3) and (9), we obtain

$$\frac{\Delta\beta_I}{\beta_I} = (2\lambda - 2.33)\frac{\Delta R}{R_{p1}}. \qquad \ldots (20)$$

In deriving Eq (20) we have assumed that the increased plasma current does not affect $\bar{p}$; this is reasonable since the ratio of jump time (10 μs) to ohmic heating time (0.5 msec) is of order 1/50. From Eq (2)

$$\Delta\Phi = \tfrac{1}{2}\frac{\Delta R}{R_{p1}} + \Delta\beta_I + \tfrac{1}{2}\Delta\ell_i, \qquad \ldots (21)$$

hence substituting for $\Delta\beta_I$, we find that

$$\chi = \beta_I (2\lambda - 2.33) + 0.5 \qquad \ldots (22)$$

and

$$\alpha = \tfrac{1}{2} \Delta \ell_i . \qquad \ldots (23)$$

(c) <u>Change in Plasma Current</u>

On the basis of flux conservation, we now express λ in terms of the physical parameters relating to state 1. The total poloidal flux linking the plasma in the initial state Ψ_1, is given by

$$\Psi_1 = L_1 I_{p1} + M_1^{vert} I^{vert} + M_1^{prim} I^{prim} + M_1^{hex} I^{hex} \qquad \ldots (24)$$

where L_1 is the plasma inductance[3]

$$L_1 = \mu_o R_{p1}\left(\ell n \frac{8R_{p1}}{a_1} + \frac{\ell_{i1}}{2} - 2\right), \qquad \ldots (25)$$

and M_1^{vert}, M_1^{prim} and M_1^{hex} are the mutual inductances between the plasma and the vertical field, primary and hexapole circuits, respectively. Here, ℓ_i is defined as $2\int_o^a B_\theta dr/(a\, B_\theta(a))$: the difference between this and Eq (4) is unimportant in the present analysis.

The currents in the external circuits, namely I^{vert}, I^{prim} and I^{hex}, are taken to be constant during the transition. This is justified, since for the largest jumps observed, these currents remain unchanged to within 5%. Using expressions of the form

$$M_2 - M_1 = \left.\frac{\partial M_1}{\partial R}\right|_{R = R_{p1}} \Delta R \qquad \ldots (26)$$

for all coefficients of mutual inductance, it is straightforward to derive

$$\frac{\Delta I_p}{I_{p1}} = - \frac{\Delta R}{R_{p1}} \left[1 + \frac{\frac{1}{2} + \frac{T}{\mu_o I_{p1}} + \frac{R_{p1}}{2} \frac{\Delta \ell_i}{\Delta R}}{\ell n\left(\frac{8R_{p1}}{a_1}\right) + \frac{\ell_{i1}}{2} - 2} \right] \qquad \ldots (27)$$

where we have used Eq (18), and T is defined by

$$T = I^{vert} \frac{\partial M^{vert}}{\partial R} + I^{prim} \frac{\partial M^{prim}}{\partial R} + I^{hex} \frac{\partial M^{hex}}{\partial R}, \qquad \ldots (28)$$

the derivatives being evaluated at $R = R_{p1}$. Now

$$I^{vert} \left. \frac{\partial M_1^{vert}}{\partial R} \right|_{R_{p1}} = 2\pi \, R_{p1} \, B_{z1}^{vert} \qquad \ldots (29)$$

with similar expressions for the other terms on the right hand side of Eq (28). For TOSCA, in the vicinity of R_o, the components are such that $B_z^{vert} >> B_z^{prim}, B_z^{hex}$, and hence using Eq (1) we find $T \simeq - \frac{1}{2}\mu_o \Phi_1 I_{p1}$. Thus we obtain

$$\lambda = 1 + \frac{\frac{1}{2} - \frac{1}{2} \Phi_1 + \frac{1}{2} R_{p1} \frac{\Delta \ell_i}{\Delta R}}{\ell n\left(\frac{8R_{p1}}{a_1}\right) + \frac{\ell_{i1}}{2} - 2} \qquad \ldots (30)$$

3. EXPERIMENTAL RESULTS

We now review the experimental work upon which our theoretical model is based. Experiments with triangular equilibria show that inward pointing plasmas ($I_h/I_p < 0$) are much easier to control than outward pointing plasmas ($I_h/I_p > 0$). This can be quantified by studying the magnitude of any displacements of the plasma major radius which occur. Figure 1 shows the possible operating regimes in the I_h/I_p (triangularity) and R_p (position) parameter space; shaded areas are inaccessible. Plasmas positioned more than 2 cm away from the vacuum vessel centre are unstable, and this is thought to be due to wall or limiter contact. There are also regions in which the plasma moves vertically up or down, the growth rate being typically $\sim$ 100 μs. These axisymmetric instabilities can be controlled by suitably positioned conductors connected in parallel as a passive feedback system[5]. Figure 1 also indicated the regions in which the horizontal jumps occur, often accompanied by a vertical axisymmetric instability. The shaded area representing this region applies to jumps of order 1 cm or greater. Whereas this horizontal motion occurs on a timescale $\sim$ 10-100 μs, any accompanying vertical motion is slower ($\gtrsim$ 100 μs). It is seen that this restriction to the operating regime applies to outward pointing plasmas only, and limits the value of I_h/I_p; thus for a plasma positioned at the hexapole centre, we have $\frac{I_h}{I_p} \lesssim 0.2$. This phenomenon can only be avoided by positioning the plasma well inside the vessel centre, and thus the hexapole centre. In this case, the resulting plasmas are no longer triangular, but become vertical ellipses which are unstable to up-down motions. The inward jumps thus inhibit the formation of outward pointing triangular plasmas. Outward pointing plasmas, positioned inside the vacuum vessel centre, are also found to move outwards. However, this motion is exponential in time ($\tau \sim$ 50-100 μs), and is due to an axisymmetric instability.

Figure 3 shows a set of experimental data obtained for an outward pointing plasma with $I_h/I_p \sim 0.3$, and positioned approximately 1.0 cm outside the vessel centre. Figures 3a and 3b show the plasma and hexapole currents respectively. Figures 3c and 3d show the horizontal (ΔR) and vertical (Δz) displacements of the plasma from the vacuum vessel centre. At t $\sim$ 2.5 ms, the plasma jumps inwards by about 2 cm, there follows a slow upward displacement together with a fast increase in plasma current. The new equilibrium position is maintained for a time of order 2 ms (~ 5 energy confinement times) before a major disruption terminates the discharge. It is this jump phenomenon which we shall attempt to interpret in terms of our theoretical model. Figure 3e shows the major radial displacement on an expanded time base. The jump shown occurs in two parts; the first part has a characteristic time ~ 10 μs and the second has a time ~ 50 μs. No oscillations about the new equilibrium position are observed. Jumps often occur on the fast time scale only. Some jumps are preceded by a low amplitude poloidal field fluctuation $\left(\left.\frac{\Delta B_\theta}{B_\theta}\right|_{r = a} \lesssim 1\%\right)$ which we accredit to m = 2, n = 1 tearing modes. Others accompany a voltage change in the primary circuit, following the switching of extra capacitance. For still others, however, the diagnostics show no sign of a trigger mechanism. We can find no dependence on the safety factor at the plasma boundary.

Figure 4 shows the variation of $\Delta I_p/I_{pl}$ for outward pointing plasmas versus the magnitude of the accompanying jump $\Delta R/R_{pl}$. The gradient, $\lambda = - \Delta I_p R_{pl}/(\Delta R I_{pl})$, lies between 0.6 and 1.2.

We now summarise the experimental results which relate $\Delta R/R_{pl}$ to I_h/I_{pl}. These can be conveniently categorised in terms of the initial plasma position and the method of triggering. We begin by considering plasmas initially situated on or outside the vessel centre ($R_{pl} \geqslant R_o$) and triggered by low-level fluctuations. The results for this case (crosses) are as shown in Figure 5. Jumps occurring for inward pointing plasmas (I_h/I_{pl} negative) are approximately independent of the initial position, whereas those for outward pointing plasmas (I_h/I_{pl} positive) vary between 2 mm and 3 cm (R_{pl} varying from 30 to 32 cm). For $I_h/I_{pl} = 0$, the scatter resulting from a large number (~ 30) of discharges is indicated by the error bars. The theoretical curves shown are discussed in Section 4. Jumps triggered by primary voltage changes tend to be larger.

For plasmas initially situated inside the vessel centre ($R_{pl} < R_o$) the jumps are small ($\lesssim$ 5 mm) and independent of the hexapole current. Some discharges are produced with no jumps at all, although the usual triggers are present.

4. DISCUSSION

a) Determination of Coefficients

In Section 2 we derived an expression (Eq 14) for the magnitude of the jump in terms of the coefficients A, B and C; we now evaluate the parameters comprising them. The coefficient B depends on R_{pl}/R_o which we treat as a variable. Thus we determine the size of the jump as a function of different initial positions.

As previously stated, the experimental values of λ lie between 0.6 and 1.2. In fact, the lower value is the theoretical limit $\Delta\ell_i \to 0$ with flux being conserved; for inward jumps this implies that experimental values of $\Delta\ell_i$ are negative.

The value of χ (Eq (22)) must be determined from β_I. This is found from toroidal flux loop measurements to be between 0.4 and 0.7. The value of Φ_1 (Eq (2)) is also required, and this is computed from the field necessary to maintain the initial equilibrium; we find that $\Phi_1 \sim 2.8 \pm 0.3$. The decay index n of the field produced by the vertical field windings is 0.6. We evaluate the field ratios by fitting the analytic expressions (Eqs (5) and (6)) to the fields (see Fig. 2) computed from the measured winding currents. Then from Figure 2b and Eq (5)

$$\frac{B_z^h}{B_{z1}^{vert}} = - 25\ I_h/I_p \qquad \ldots (31)$$

and from Figure 2c and Eq (6)

$$\frac{B_z^e}{B_{z1}^{vert}} = - 1.36\ I_h/I_p. \qquad \ldots (32)$$

Setting $\lambda = 0.8$, the coefficients A and B can now be expressed in terms of I_h/I_{p1} and R_{p1}/R_o, that is

$$A = - 25\ I_h/I_{p1} \qquad \ldots (33)$$

and $$B = - 1.36\ I_h/I_{p1} - 50\,\frac{I_h}{I_{p1}}\left(\frac{R_{p1}}{R_o} - 1\right) + 1.15 \qquad \ldots (34)$$

We now determine the last coefficient, C (Eq (14)), which represents the trigger mechanism for the jump. This is obtained by fitting the analytic and experimental values of $\Delta R/R_{p1}$ for a circular plasma ($I_h/I_{p1} = 0$): $\Delta R/R_{p1} = - C/B$. The dependence of $\Delta R/R_{p1}$ on I_h/I_{p1} then becomes the test of the model. From Figure 5 we obtain C = 0.012, which given flux conservation, implies $\Delta \ell_i = - 0.07$. This is equivalent to a flattening of the current profile consistent with the proposed trigger mechanism.

b) Results

The curves in Figure 5 represent the analytic dependence of $\Delta R/R_{p1}$ on I_h/I_{p1} (Eq (14)), with the values of A, B and C determined as described above. Results are shown for $(R_{p1}/R_o - 1) = 0.07$ and 0.0, corresponding to plasmas initially 2.1 cm outside the vessel centre, and at the centre.

For each value of $(R_{pl}/R_o - 1)$ there are two branches corresponding to the two solutions (±) represented by Eq (14). For inward pointing plasmas, $I_h/I_{pl} < 0$, two inward displacements (inwardly displaced equilibria) are predicted. For outward pointing plasmas, $I_h/I_{pl} > 0$, both an inward and outward displacement are predicted. For a circular plasma, $I_h/I_{pl} = 0$, a small inward (negative solution) and an infinite (positive solution) displacement are predicted. It is this small inward displacement which is fitted to the experimental jump to determine C.

The experimental results are all inward jumps. For inward pointing plasmas there is agreement between the experiment and the smaller of the predicted displacements. For outward pointing plasmas the experimental values are within the range predicted for the different initial positions. Although outward displacements are also predicted, none are observed experimentally. Generally, the jumps for inward pointing plasmas are slightly less than predicted, whereas those for outward pointing plasmas are slightly larger.

The agreement between experiment and theory shows that the jump phenomenon which is observed to limit the maximum triangularity can be explained as the motion between two equilibria following a perturbation to the plasma parameters. In most cases the equilibrium position to which the plasma jumps corresponds to the negative solution of Eq (14): that is, the state which is a modification of the initial one. Jumps to the neighbouring equilibrium (positive solution) have not been definitely identified, the possible solutions being difficult to distinguish in some experiments.

Although the analytic and experimental values of $\Delta R/R_{pl}$ are in good agreement for plasmas positioned either outside or on the vacuum vessel (and hexapole) centre, this is not the case for plasmas initially positioned inside the vessel centre ($R_{p1} < R_o$). In order to simulate this situation, suppose the plasma minor radius to be reduced by loss of plasma through contact with the wall. Such an adjustment, which is supported by the qualitative physical arguments, leads to much better agreement between theory and experiment.

We now consider the important question of energetics. Intuitively, we expect that a flux conserving plasma would seek to lower its potential energy by expanding in major radius. A detailed study of the entire plasma and magnetic energy confirms this view. We therefore conclude that an inward jump must be associated with a loss of flux. Thus it is necessary for us to correct the derivations of λ, α and χ. Denoting the changes in poloidal and toroidal fluxes by $\Delta\Psi$ and $\Delta\Psi_{tor}$, respectively, then it can be deduced that

$$\lambda = 1 + \frac{\frac{1}{2} - \frac{1}{2}\Phi_1 + R_{p1}\frac{\alpha}{\Delta R} - \frac{R_{p1}}{\Delta R}\left[\frac{\Delta\Psi}{\mu_o I_{p1} R_{p1}} - \frac{2}{3\pi}\beta_I \frac{\Delta\Psi_{tor}}{B_o a^2}\right]}{\ell n\left(\frac{8R_{p1}}{a_1}\right) + \frac{\ell_{i1}}{2} - 2} \qquad \ldots (35)$$

where B_o is the toroidal field at the centre of the hexapole. The parameter χ is unaffected, but α is now given by

$$\alpha = \frac{\Delta\ell_i}{2} - \left(1 + \frac{4\beta_I}{3}\right) \frac{\Delta\Psi_{tor}}{2\pi B_o a^2} \qquad \ldots (36)$$

This reinterpretation of α does not affect our previous determination of C. As before $\alpha < 0$, and substitution of typical experimental values into Eq (35), leads to

$$\Delta\Psi < \frac{2\beta_I}{3\pi} \frac{\mu_o I_{pl} R_{pl}}{B_o a^2} \Delta\Psi_{tor} \qquad \ldots (37)$$

Since we have argued that an inward jump cannot occur with flux conservation, and the above condition forbids $\Delta\Psi = 0$ and $\Delta\Psi_{tor} < 0$, then it follows that $\Delta\Psi < 0$, that is, poloidal flux must be lost.

Thus the observations and analysis of this paper suggest two tentative interpretations. In the case of two neighbouring equilibria, their apparent MHD stability prior to, and following the jump, implies that in some sense the plasma moves from one 'well' to another; this further implies the existence of an intermediate 'hill'. A dissipative mechanism involving a change in ℓ_i and a loss of magnetic flux, conceivably allows the plasma to access the inner 'well'. For this motion to occur, of course, the minimum of the inner 'well' must be lower than that of the outer. Alternatively, the plasma occupies a 'well' which subject to changes in ℓ_i and loss of flux, leads to a modified equilibrium. The latter, presumably, being a 'well' of lower minimum and displaced inwards.

We now relate the results presented here to other machines. Most present and future non-circular tokamaks include both triangularity and ellipticity. We have computed such equilibria, including the ellipticity by changing the decay index, n, in Eq (12). A large negative decay index simulates a vertical ellipse, while a positive value simulates a horizontal ellipse. The results can be summarised as follows. For both outward and inward facing D's, the jumps will be very small ($|\Delta R/R| \lesssim 0.003$). For pear shapes pointing inwards, loss of equilibria is predicted (when flux is conserved). For pear shapes pointing outwards, large jumps are predicted ($|\Delta R/R| \gtrsim 0.2$). Regarding existing machines, none have yet operated under conditions where large jumps are predicted.

5. CONCLUSIONS

Experimental observations on axisymmetric jumps in a hexapole tokamak have been described. This phenomenon restricts the possible triangularity of the plasma cross-section. In particular, outward pointing plasmas with a triangularity sufficient to stabilise internal modes cannot be produced in TOSCA.

A theoretical model has been described which interprets the jump as the transition between two equilibrium states. It is assumed that the maintaining poloidal field is provided by fixed currents in external conductors, with the plasma current adjusting inductively. Following a small perturbation to the plasma parameters, two new equilibrium positions are shown to exist. One of these corresponds to a modification of the initial equilibrium due to the parameter change, which in the present paper we take to be the self-inductance. The other solution represents a second equilibrium position neighbouring the initial state, and which a change in self-inductance renders accessible. Our theory gives the dependence of the magnitude of the jump on the hexapole field (or triangularity) and the initial plasma position. We have shown the jumps to be consistent with a loss of poloidal flux.

Good agreement between the predictions of the model and the experiment are found for plasmas initially outside the vacuum vessel (or hexapole) centre. In most cases the jump is to the modified, rather than the neighbouring equilibrium. For plasmas initially positioned inside the centre, however, theory and experiment are in disagreement. This discrepancy can be explained by assuming that the radius is reduced when the plasma touches the inside wall.

ACKNOWLEDGEMENTS

We thank the TOSCA team for experimental assistance, in particular Dr. D.C. Robinson and K. McGuire. We also thank Dr. D.C. Robinson for useful suggestions.

REFERENCES

(1) BUSSAC, M.M., EDERY, D., PELLAT, R. and SOULE, J.L., in Plasma Physics and Controlled Nuclear Fusion Research, Berchtesgaden 1976, IAEA Vienna, 1 (1977) 607.

(2) McGUIRE, K., ROBINSON, D.C. and WOOTTON, A.J., in Plasma Physics and Controlled Nuclear Fusion Research, Innsbruck 1978, IAEA Vienna, 1 (1979) 335.

(3) MUKHOVATOV, V.S. and SHAFRANOV, V.D., Nuclear Fusion 11 (1971) 605.

(4) THOMAS, C.Ll., The numerical calculation of axisymmetric MHD equilibria in discrete conductor configurations, Computational methods in Classical and Quantum Physics, (Ed. M.B. Hooper), Transcripter Books, 1977.

(5) ROBINSON, D.C. and WOOTTON, A.J., Nuclear Fusion 18 (1978) 1555.

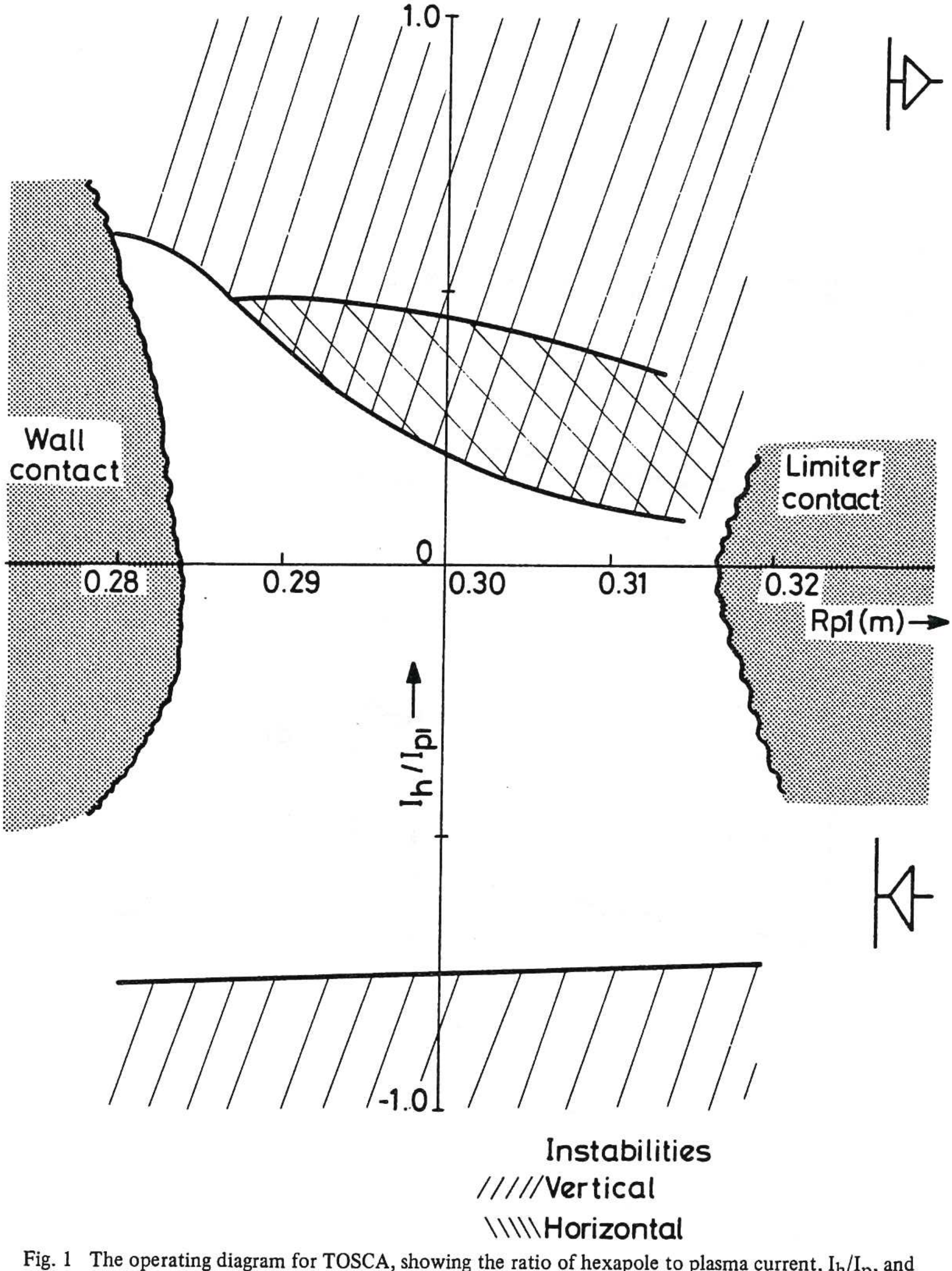

Fig. 1 The operating diagram for TOSCA, showing the ratio of hexapole to plasma current, I_h/I_p, and position R_p, at which satisfactory equilibria are obtained. The shaded areas are inaccessible because of (i) vertical axisymmetric instabilities, (ii) wall contact or (iii) the horizontal jumps.

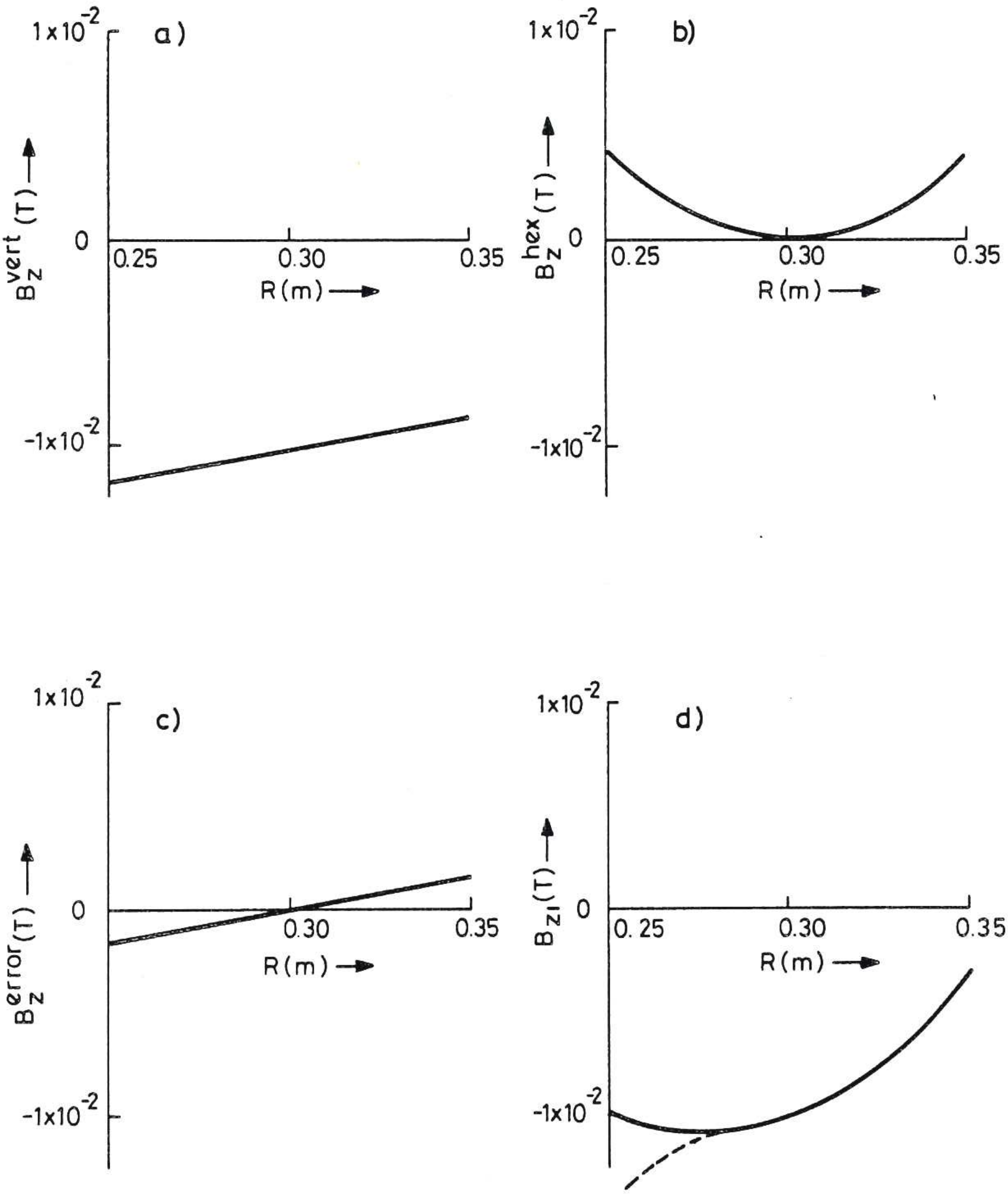

Fig. 2 The magnetic field components used in the theoretical model which comprise the total vertical equilibrium maintaining field. (a) the field from the vertical field windings, (b) the hexapole field from the hexapole windings, (c) the error field from the hexapole windings, (d) the total field for $I_h/I_p \simeq 0.6$. The broken line in Fig. 2(d) represents the actual field in the experiment.

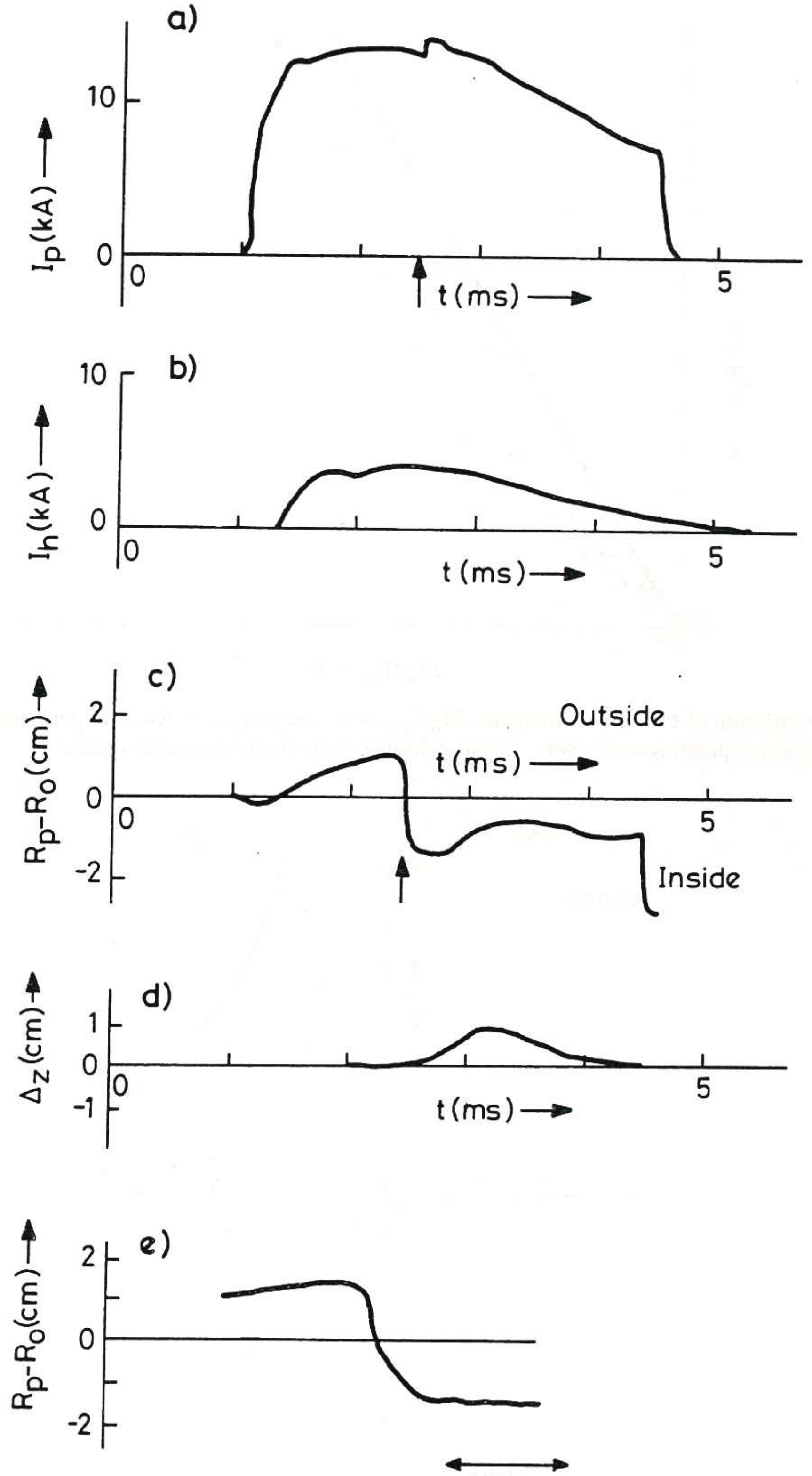

Fig. 3 Experimental data for an outward pointing plasma (a) the plasma current, (b) the hexapole current, (c) the horizontal displacement of the plasma electrical centre from the vacuum vessel centre (R_o = 30 cm), (d) the vertical displacement of the plasma electrical centre from the vacuum vessel centre, (e) the horizontal displacement in the vicinity of the jump, on an expanded time scale.

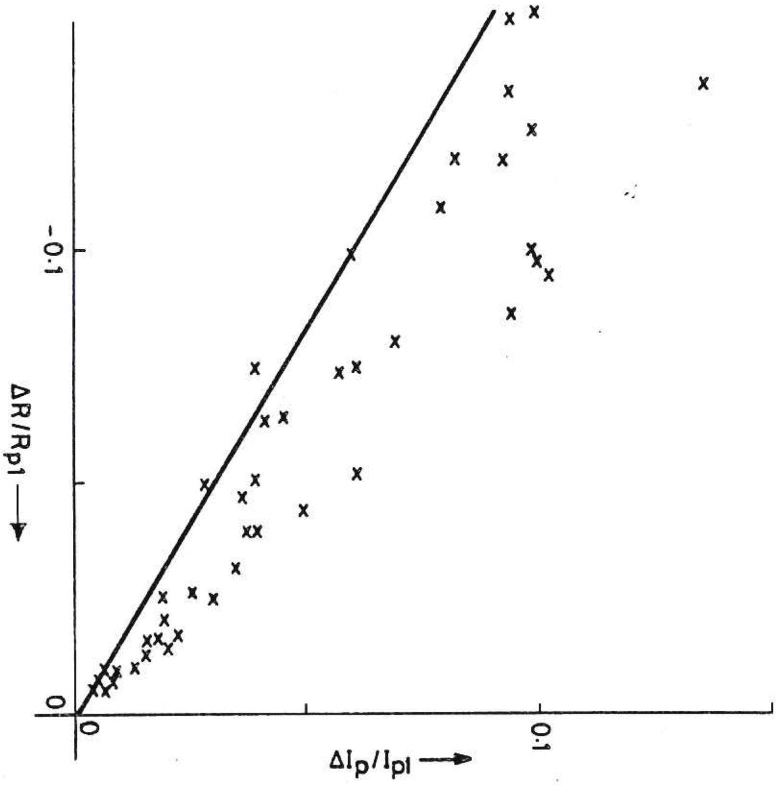

Fig.4 The variation of the current increase, $\Delta I_p/I_{p1}$, with the jump, $\Delta R/R_{p1}$. Experimental jumps for outward pointing plasmas are shown. The straight line is the theoretical dependence.

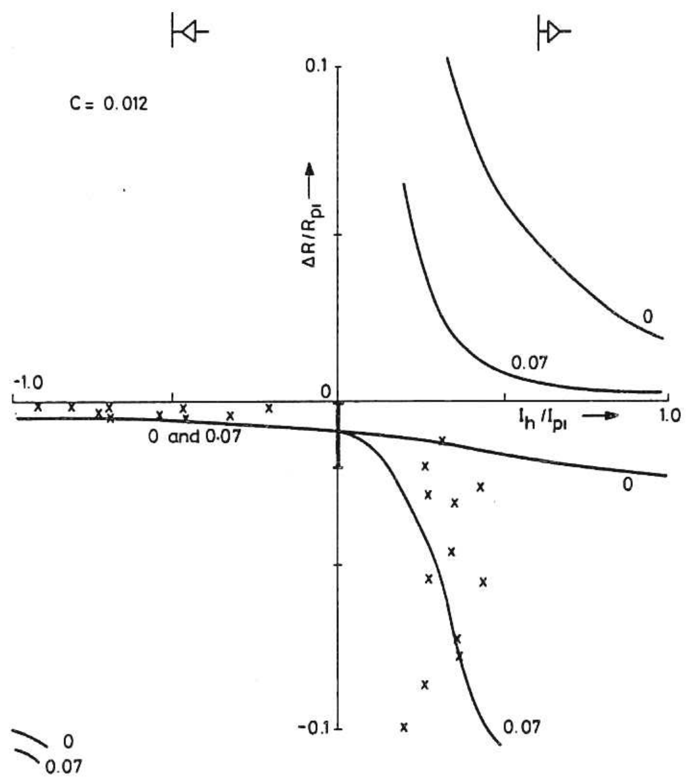

Fig. 5 The dependence of the jump, $\Delta R/R_{p1}$, on the ratio of hexapole to plasma current, I_h/I_{p1}, for plasma positioned outside the vessel centre exhibiting no, or very low, field fluctuations. The lines represent the theoretical dependence for plasmas initially on the centre (labelled $(R_{p1}/R_o - 1) = 0$), or 2.1 cm outside (labelled $(R_{p1}/R_o - 1) = 0.07$).